# Tissue-Specific Inactivation of Type II Deiodinase Reveals Multi-Level Control of Fatty Acid Oxidation by Thyroid Hormone in the Mouse

Tatiana L. Fonseca[1*], Joao Pedro Werneck-De-Castro[1,2*], Melany Castillo[1], Barbara M. L. C. Bocco[1], Gustavo W. Fernandes[1], Elizabeth A. McAninch[1], Daniele L. Ignacio[1,2], Caio C. S. Moises[1], Alexandre Ferreira[1], Balázs Gereben[3]and Antonio C. Bianco[1]

[1]Division of Endocrinology, Diabetes and Metabolism, University of Miami Miller School of Medicine, Miami, Florida
[2] Biophysics Institute and School of Physical Education and Sports, Federal University of Rio de Janeiro, Rio de Janeiro, Brazil.
[3]Department of Endocrine Neurobiology, Institute of Experimental Medicine, Hungarian Academy of Sciences, Budapest, H-1083 Hungary

**Keywords:** Deiodinases; thyroid hormone; cold acclimatization; fatty acid oxidation

**Running title**: Regulation of Fatty Acid Oxidation by Thyroid Hormone

[*] These authors contributed equally to this manuscript

**Corresponding author:**

Antonio C. Bianco, MD, PhD
University of Miami Miller School of Medicine,
1400 N.W. 10th Avenue, Suite 601
Miami, Florida 33136, USA
Phone: 305.243.5631; Fax: 305 243 7268;
E-mail: abianco@deiodinase.org



Diabetes Publish Ahead of Print, published online January 31, 2014

The type 2 deiodinase (D2) converts the pro-hormone T4 to the metabolically active molecule T3, but its global inactivation (GLOB-D2KO) unexpectedly lowers the respiratory exchange rate (RQ) and increases food intake. Here we used FloxD2 mice to generate systemically euthyroid FAT-specific (Fabp4-Cre), ASTROCYTE-specific (GFAP-Cre) or SKELETAL MUSCLE-specific (MLC-Cre) D2KO mice that were monitored continuously. The ASTRO-D2KO mice also exhibited lower diurnal RQ and greater contribution of fatty acid oxidation to EE, but no differences in food intake were observed. In contrast, the FAT-D2KO mouse exhibited sustained (24 h) increase in RQ values, increased food intake, tolerance to glucose and sensitivity to insulin, all supporting greater contribution of carbohydrate oxidation to EE. Furthermore, FAT-D2KO animals that were kept on a high-fat diet for 8 weeks gained more body weight and fat, indicating impaired brown adipose tissue (BAT) thermogenesis and/or inability to oxidize the fat excess. Acclimatization of FAT-D2KO mice at thermoneutrality dissipated both features of this phenotype. Muscle D2 does not seem to play a significant metabolic role given that SKM-D2KO animals exhibited no phenotype. The present findings are unique in that they were obtained in systemically euthyroid animals, revealing that brain D2 plays a dominant albeit indirect role in fatty acid oxidation via its sympathetic control of BAT activity. D2-generated T3 in BAT accelerates fatty acid oxidation and protects against diet-induced obesity.

## Introduction

Thyroid hormone signaling is initiated by entry of 3,5,3'-triiodothyronine (T3) into target cells and binding with nuclear T3-receptors (TR), modulating the expression of T3-responsive genes (1). Signaling through this pathway is also affected by local events, with target cells playing a role through controlled expression of the activating or inactivating deiodinases (2). These enzymes are thyroredoxin fold-containing selenoproteins that can activate the pro-hormone thyroxine (T4) to its active form T3 (type II deiodinase: D2) or inactivate both T4 and T3, and T3 to T2 (type III deiodinase: D3) (3-5). As a result, cells that express D2 have higher T3 levels and thus exhibit an enhanced T3-dependent mRNA footprint, and the opposite is observed in D3-expressing cells. Thus, customizing thyroid hormone signaling via deiodinases is an important mechanism in energy homeostasis (2), brain (6), brown adipose tissue (BAT) (7), pancreatic β-cell (8), heart (9) and skeletal muscle (10, 11).

Inactivation of the D2 gene (Dio2) affects the expression of T3-dependent genes in D2-expressing tissues such as BAT and brain, essentially dampening thyroid hormone signaling in a tissue-specific fashion (12). Accordingly, a mouse with global inactivation of the Dio2 gene (GLOB-D2KO) exhibits a significant metabolic phenotype characterized by decreased RQ, resistance to diet-induced obesity and super tolerance to glucose, some of which is reversed upon acclimatization at thermoneutrality (13). A similar phenomenon was observed in the UCP1-KO mouse (14) and in systemically hypothyroid mice (15). These findings indicate that an increase in sympathetic activity at room temperature plays a role in defining the metabolic phenotype of animal models exhibiting a disruption in thyroid hormone signaling, either localized (GLOB-D2KO) or systemic (16, 17).

D2-generated T3 has been shown to play a critical role in BAT UCP-1 expression (18, 19) and BAT thermogenesis (20). Thus, the metabolic phenotype displayed by the GLOB-D2KO mouse has been largely attributed to the lack of D2-generated T3 in BAT (13, 21, 22). In fact, BAT D2 is induced by sympathetic activity and rapidly increases thyroid hormone signaling during cold exposure (23, 24). However, a number of other metabolically relevant tissues in the rodent express D2, e.g. brain (25), skeletal muscle (26), bone (27), and could also play a role in defining the metabolic phenotype of the GLOB-D2KO mouse. For example, D2 is expressed in the medi-obasal hypothalamus (28, 29) where it has been implicated in the orexigenic response during re-feeding (30) and in lowering TRH/TSH secretion in disease states (31). At this time, it is still not clear what, if any, metabolic roles D2 plays in skeletal muscle and bone.

The lower RQ observed in the GLOB-D2KO animals is unexpected because thyroid hormone administration is known for accelerating fatty acid oxidation (32) and lowering RQ values (33). However, given that the lower RQ values are dissipated once the GLOB-D2KO animals are acclimatized to thermoneutrality (13), it is likely that a compensatory increase in BAT sympathetic activity plays a role (16, 17). Of note, a subsequent study did not find a lower RQ in the GLOB-D2KO mouse studied briefly by indirect calorimetry (34), despite reduced liver glycogen and elevated serum βOH-butyrate levels, which is commonly associated with increased sympathetic activity and fatty acid oxidation (35).

The present studies were performed to define the mechanism(s) and anatomical site(s) whereby D2-mediate T3 production affects fatty acid oxidation as reflected in the RQ. To this aim, we compared the metabolic phenotype of the GLOB-D2KO mouse with that of three other systemically euthyroid mouse strains that exhibit (i) astrocyte-specific (ASTRO-D2KO), (ii) fat-specific (FAT-D2KO) or (iii) skeletal muscle-specific (SKM-D2KO) inactivation of Dio2 after they were admitted to a comprehensive lab animal monitoring system (CLAMS) and monitored continuously through indirect calorimetry. Our findings indicate that brain D2 indirectly inhibits BAT fatty acid oxidation via dampening of sympathetic activity in BAT. In contrast, D2-generated T3 in BAT accelerates fatty acid oxidation given that selective disruption of this pathway in BAT increases RQ and predisposes to diet-induced obesity. No significant metabolic phenotype resulting from D2 inactivation in skeletal muscle was identified. The evidence obtained through the use of these animal models is unique in its physiological relevance because it reflects the result of tissue-specific D2 inactivation in an otherwise systemically euthyroid animal.

## Material and Methods

### *Animals*

All experimental procedures were planned following the American Thyroid Association guide to investigating thyroid hormone economy and action in rodent and cell models (36), and approved by the local Institutional Animal Care and Use Committee. For the studies including the GLOB-D2KO mouse, approximately 10 weeks old C57BL/6J and GLOB-D2KO mice that had been backcrossed in the same background (22) were used from our established colonies, kept at room temperature (22°C), with a 12-h dark/light cycle starting at 06:00 h and housed standard plastic cages with four male mice per cage.

For the tissue specific deletion of *dio*2 in adipose tissue, astrocytes and skeletal muscle cells, we establish an *in vivo* mouse model for cell-type specific deletion of D2 generating floxed D2 (*dio*2$^{Flx}$) mice as described (37). The *dio*2$^{flx}$ mice were crossed with transgenic mice expressing Cre-recombinase under the fatty acid binding protein 4 promoter (Cre-FABP4) [B6.Cg-Tg(Fabp4-cre)1Rev/J; Jackson Laboratories, Bar Harbor ME] (38) or glial fibrillary acidic protein promoter (Cre-GFAP) [FVB-Tg(GFAP-cre)25Mes/J; Jackson Laboratories] (39) or myosin light chain 1f (Cre-MLC) (40). This strategy was used in order to eliminate D2 activity in the Fabp4- expressing adipocytes (FAT-D2KO mice), GFAP-expressing astrocytes (ASTRO-D2KO mice) and MLC-expressing myocytes (SKM-D2KO). In all experiments only Cre littermates were used as controls. The generation of the Astro-D2KO mice was recently described (37). At the time of the studies all mice were between 9 and 14 weeks of age.

Only male animals were used. Animals were kept on standard chow diet (3.1kcal/g) (2918 Teklan Global Protein rodent diet, Madison, WI) or a high fat diet (4.5kcal/g) (TD 95121; Harlan Teklad, Indianapolis, IN) as indicated. In the experiments involving the high fat feeding three month-old littermate controls and FAT-D2KO or SKM-D2KO mice (6 per group) that had been fed chow diet were switched to a high fat diet for 8 weeks, kept at room temperature (22°C) or thermoneutrality (30°C) as indicated.

At the end of experimental period the animals were euthanized by asphyxiation in a $CO_2$ chamber. Blood was collected and serum levels of TSH, T4 and T3 measured using a MILLIPLEX$^{TM}$ rat thyroid hormone panel kit following the instructions of the manufacturer (Millipore Corporation, Billerica MA) and read on a BioPlex (BioRad, Hercules CA).

### *Body composition*

Lean body mass (LBM) and fat mass were determined by dual energy x-ray absorptiometry (DEXA; Lunar Pixi, Janesville, WI) as described previously (13).

### *Indirect calorimetry*

Animals were admitted to a comprehensive lab animal monitoring system (CLAMS - OXYMAX System 4.93 - Columbus Instruments, Columbus, OH) (13) with free access to food and water. Studies were performed at 22°C, 18°C, 15°C, 11°C and 5°C for the indicated times. Animals were allowed to acclimatize in individual metabolic cages for 48 h before any measurements. Subsequently, metabolic profiles were generated as indicated and the data collected in the next 36 h. This system allows for continuous measurement of Oxygen consumption ($VO_2$; ml/kg

BW/h) and carbon dioxide production ($VCO_2$) in successive 14 or 26-min cycles, using a sensor calibrated against a standard gas mix containing defined quantities of $O_2$ and $CO_2$. These data were used to calculate the respiratory exchange ratio (RQ) ($VCO_2/VO_2$) and the Energy Expenditure (EE) ([3.815+1.232●RQ]●$VO_2$). Contribution of fat acid oxidation to energy expenditure (EE) was calculated as described using the following equation: % fat contribution = (468.6●(1-RQ))/(5.047●(RQ-0.707)+4.686●(1-RQ) (41). 24 h caloric intake was measured at the indicated times while the animals were admitted to the CLAMS.

***Glucose and insulin tolerance tests***

For glucose tolerance tests, mice were fasted overnight and the glucose measurement was made as described previously (42). For insulin tolerance tests, mice with food *ad libitum* were injected with insulin and the glucose measurement was made as described previously (42).

***Deiodinase assays***

D2 activity assay was performed in BAT sonicates as described previously (43, 44).

***Statistical analysis***

All data are expressed as mean ± SEM and were analyzed using PRISM software (GraphPad Software, San Diego, CA). One-way ANOVA was used to compare more than two groups, followed by the Student-Newman-Keuls test to detect differences between groups. The Student's t test was used only when two groups were part of the experiment. $P<0.05$ was used to reject the null hypothesis.

## Results

### *GLOB-D2KO mice exhibit increased diurnal fatty acid oxidation*

Under the mild thermal stress conditions of room temperature (22˚C), all animals exhibited the expected circadian rhythmicity in $VO_2$ and EE with higher values observed nocturnally, when animals are awake and eating, as opposed to the day-hours, when the animals are resting and eating much less (Fig. 1A; supplemental Fig. 1A). In this setting, no differences were observed between GLOB-D2KO and WT animals (Fig. 1A). The RQ profile also exhibited circadian rhythmicity with lower values observed diurnally (Fig. 1B). Notably, the diurnal decrease in RQ values was more pronounced in the GLOB-D2KO animals (Fig. 1B), resulting in greater contribution of fatty acid oxidation to the diurnal EE (~50% vs. ~35 %; Fig. 1C). This diurnal drop in RQ was associated with a ~50 % reduction in diurnal food intake in the global-D2KO animals, with no differences observed nocturnally (Fig. 1D).

The association between reduced food intake and increased fatty acid oxidation in the GLOB-D2KO animals suggest an involvement of the central nervous system, presumably the hypothalamus. Thus, we next tested whether the differences between GLOB-D2KO and WT animals would be dissipated in the setting of intense hypothalamic-driven fatty acid mobilization and oxidation, i.e. cold exposure. Housing for 24 h at 4°C resulted in dramatic increase in $VO_2$ and EE in all animals that blurred circadian rhythmicity, similar in GLOB-D2KO and WT controls (Fig. 1E; supplemental Fig. 1B). In contrast, the RQ profile exhibited the expected circadian rhythmicity in both groups of animals but the diurnal RQ difference between GLOB-D2KO and WT controls was dissipated (Fig. 1F). This equalized the contribution of fatty acid oxidation to diurnal EE (Fig. 1C). In this setting, both diurnal and nocturnal food intake were similar in all animals (Fig. 1G). Similar findings were obtained when the environment temperature was gradually and progressively decreased every 3 days while the animals remained in the CLAMS for a 2-week period, except that in this case the $VO_2$ circadian rhythmicity was preserved throughout the experiment (Fig. 1H-I).

Decreasing BAT's contribution to metabolism by acclimatization to thermoneutrality normalized the RQ in the GLOB-D2KO mouse (13). Thus, in the next set of experiments we used an alternative strategy to decrease BAT's contribution to metabolism, i.e. fasting. In fact, a 48 h fasting dramatically reduced $VO_2$ and EE while it minimized their circadian rhythmicity (Fig. 1J; supplemental Fig. 1C). Furthermore, fasted GLOB-D2KO and WT controls markedly lowered their RQ values, and the 24-profile lost circadian rhythmicity (Fig. 1K). These changes in RQ elevated the contribution of fatty acid oxidation to diurnal EE to almost 80 % in all animals (Fig. 1C). More importantly, such as with cold exposure, fasting also dissipated the diurnal differences in RQ between GLOB-D2KO animals and WT controls (Fig. 1K).

### *Astro-D2KO mice partially recapitulate the metabolic phenotype of the GLOB-D2KO animals*

It has been proposed that D2-generated T3 in glial cells near the arcuate nucleus play an orexigenic role in mice (45, 46). Thus, to test whether the lower diurnal RQ observed in GLOB-D2KO mouse is caused by D2 inactivation in the brain we studied the ASTRO-D2KO mouse that lacks D2 activity in the glia but preserves D2 expression in other tissues/cells including the

ependimal tanycytes (37). These animals have normal serum levels of T4, T3 and TSH and are considered systemically euthyroid (37). The ASTRO-D2KO animals exhibit a normal growth curve (Fig. 2A) and during adulthood have similar body weight (Fig. 2B) and body composition (Fig. 2C) as compared to WT littermate controls. The CLAMS studies revealed that ASTRO-D2KO animals have a $VO_2$ and EE profiles that was unremarkable (Fig. 2D; supplemental Fig. 1D), but a RQ profile that resembled that of the GLOB-D2KO mouse, i.e. lower diurnal values (Fig. 2E), with greater contribution of fatty acid oxidation to the diurnal EE (Fig. 2F); food intake however was not different when compared to WT littermate controls (Fig. 2G).

***Fat-D2KO mice exhibit around-the-clock reduction in fatty acid oxidation***

D2 is expressed in BAT and D2-generated T3 has been shown to regulate local fatty acid synthesis (16, 47, 48). To test whether D2-generated T3 in BAT affects fatty acid oxidation we next studied FAT-D2KO mice that lack BAT D2 expression (supplemental Fig. 2A) and activity (supplemental Fig. 2B) while expressing D2 normally in other tissues (supplemental Fig. 2C). These animals have no gross abnormalities, develop and grow normally up until age 5 months, when they exhibit a slightly reduced rate of weight gain (Fig. 3A). These animals also exhibit normal serum levels of T4, T3 and TSH (supplemental Fig. 2D-F) and are considered systemically euthyroid.

Adult FAT-D2KO mice exhibit similar body weight (Fig. 3B) and body composition (Fig. 3C) when compared to littermate controls. Their $VO_2$ and EE profiles showed no differences when compared to littermate controls (Fig. 3D; supplemental Fig. 1E). However, RQ values were substantially higher in the FAT-D2KO mice across the 24 h cycle (Fig. 3E), indicating that the absence of D2 in BAT (and WAT) reduces the contribution of fatty acid oxidation to EE (Fig. 3F). It is notable that FAT-D2KO animals also exhibit greater food intake throughout the 24 h cycle (Fig. 3G), although their body weight (Fig. 3B) and body composition (Fig. 3C) are not different from WT littermate controls. The relatively greater contribution of glucose oxidation to EE was further documented through IPGTT and ITT (Fig. 3H-I). FAT-D2KO animals were more tolerant to glucose (Fig. 3H) and exhibited a greater sensitivity to insulin administration (Fig. 3I) when compared to WT littermate controls.

Given that D2 activity in WAT is minimal, these differences in RQ are likely to reflect the absence of D2 in BAT. To test if this was the case, we used similar strategy as with the GLOB-D2KO animals, i.e. to minimize BAT contribution to EE by acclimatization at thermoneutrality (30˚C for 8 weeks) or by fasting. Acclimatization at thermoneutrality resulted in significant reduction in $VO_2$ and EE, with no differences between FAT-D2KO and control animals (Fig. 3J; supplemental Fig. 1F). Notably, in this setting the RQ values for the FAT-D2KO decreased and became indistinguishable from WT littermate controls (Fig. 3K), with similar observations for food intake (Fig. 3L). At the same time, fasting dramatically reduced $VO_2$ and EE as well as their circadian rhythmicity (Fig. 3M-N; supplemental Fig. 1G). More importantly, fasting also dissipated the differences in RQ between FAT-D2KO and WT littermate controls (Fig. 3N).

***FAT-D2KO mice are more susceptible to diet-induced obesity***

Given the relative reduction in fatty acid oxidation in the FAT-D2KO BAT, we hypothesized these animals would have impaired BAT thermogenesis and therefore be more susceptible to diet-induced obesity. To test if this was the case, FAT-D2KO animals were placed on a HFD for 8 weeks and notably gained significantly more body weight than WT littermate controls (Fig. 4A-B) while exhibiting similar food consumption (Fig. 4C). In addition, at the end of the experimental period the FAT-D2KO animals had experienced a greater increase in body fat than WT littermate controls kept on the same diet (Fig. 4D-E), but the contribution of fatty acid oxidation to EE remained unaffected (Fig. 4F) and the $VO_2$, EE and RQ profiles were not different in these animals (Fig. 4G-H; supplemental Fig. 1H). Next, to confirm that the greater gain in body weight and body fat in the FAT-D2KO animals were due to impaired BAT thermogenesis, we repeated the HFD for 8 weeks while the animals were kept continuously at thermoneutrality. While food intake remained largely unaffected (Fig. 4K),both groups of animals gained body weight (Fig. 4I-J) and body fat (Fig. 4L-M) in the same proportion once BAT's contribution to EE was minimized. Furthermore, CLAMS studies indicated that $VO_2$, EE and RQ profiles as well as fatty acid contribution to EE were indistinguishable between both groups of animals (Fig. 4N-P; supplemental Fig. 1I).

***SKM-D2KO mice have neutral metabolic phenotype***

Skeletal muscle expresses low levels of D2 activity but its relatively large mass suggests that D2-generated T3 in this organ may contribute significantly to the overall metabolism. We tested if this was the case by using a mouse model that lacks D2 in the skeletal muscle but preserves D2 activity in all other tissues, i.e. the SKM-D2KO mouse (49). These animals have normal serum levels of T4, T3 and TSH and are considered systemically euthyroid (49). SKM-D2KO mice exhibit a similar growth curve as littermate controls (Fig. 5A) and, during adulthood, also exhibit similar body weight (Fig. 5B) and body composition (Fig. 5C). The $VO_2$ (Fig. 5D), EE (supplemental Fig. 1J) and RQ profiles (Fig. 5E) as well as the contribution of fatty acid oxidation to EE (Fig. 5F) showed no differences when compared to WT littermate controls; food intake was also similar between groups (Fig. 5G). Next, SKM-D2KO animals were placed on a HFD for 8 weeks to test their ability to handle an excess of calories. Remarkably, these animals exhibited similar gain of body weight (Fig. 5H-I) and fat (Fig. 5J-K) as compared to WT littermate controls, with no differences observed in the VO2 (Fig. 5L), EE (supplemental Fig. 1L) and RQ (Fig. 5M) profiles.

## Discussion

The utilization of systemically hypothyroid or hyperthyroid animals has been the traditional approach to study thyroid hormone action (36). However, almost all tissues and cells respond to thyroid hormone and set off waves of secondary and tertiary effects that are not directly regulated by thyroid hormone. Furthermore, that thyroid hormone membrane transporters, deiodinases and TR subtypes can customize thyroid hormone effects on target tissues makes the systemic approach unsuitable for the study of cell-specific thyroid hormone actions. The present studies employed a series of systemically euthyroid animal models that exhibit tissue-specific disruption of the D2 pathway and identified a multi-level physiological control of fatty acid oxidation by thyroid hormone. The present findings are unique in that the animal models used remained systemically euthyroid throughout the experiments, revealing the physiological multi-level roles played by D2-generated T3 in fatty acid oxidation.

Selective inactivation of the D2 pathway in glial cells (ASTRO-D2KO) accelerates the diurnal rate of fatty acid oxidation in the BAT (Fig. 2E). These findings are in line with the concept that localized thyroid hormone signaling in the hypothalamus and other brain areas (e.g. brain stem) regulate appetite, BAT sympathetic activity (50, 51) and downstream metabolic and cardiovascular targets (52). In contrast, inactivation of D2 in a peripheral tissue, i.e. BAT (FAT-D2KO), led to the opposite metabolic phenotype, including a slower rate of fatty acid oxidation (Fig. 3E) and increased the contribution of carbohydrate oxidation to the overall EE (Fig. 3F). FAT-D2KO mice were also susceptible to diet-induced obesity and gained more weight and body fat on a HFD (Fig. 4C-D). Notably, disruption of the D2 pathway in a second peripheral tissue, i.e. skeletal muscle, was metabolically neutral (Fig. 5A-I), an indication that D2 activity in this tissue is unlikely to play any significant metabolic role.

The RQ reflects the relative contribution of fatty acid, glucose and protein oxidation to daily energy expenditure. Given that $VO_2$ (Fig. 1A) and total daily EE (supplemental Fig. 1A) remained stable in the GLOB-D2KO animals, the lower diurnal RQ values (Fig. 1B) indicate an acceleration of fatty acid oxidation (Fig. 1C). Liver, heart, skeletal muscle and BAT all exhibit high rates of fatty acid oxidation and could play a role in this process (53). That the difference in RQ is dissipated by BAT inactivation, i.e. thermoneutrality (13) or fasting (Fig. 1J-K), identifies BAT as the most likely tissue underlying this phenotype. However, is D2-generated T3 playing a direct role in BAT by controlling local fatty acid oxidation or playing an indirect role in BAT via the central nervous system and sympathetic activity, or both?

The fact that a diurnal reduction in food intake is part of this phenotype (Fig. 1D) suggests an involvement of the central nervous system. In addition, the fact that the difference in RQ is diurnal and not across the 24 h cycle does not support a “defect” in BAT but rather an adjustment made by the sympathetic nervous system with the possible involvement of higher control areas in the brain. Accordingly, maximal sympathetic stimulation of BAT during cold exposure also dissipated the differences in RQ between GLOB-D2KO and WT controls (Fig. 1F,I).

That the mechanism leading to lower RQ values in the GLOB-D2KO mouse is centrally mediated is supported by the previous observation that BAT norepinephrine turnover is accelerated in GLOB-D2KO mice maintained at room temperature (22). For example, it has been proposed that

D2-generated T3 in the glial cells surrounding the arcuate nucleus is important for the orexigenic response during fasting, by increasing appetite and decreasing BAT activity in order to preserve energy (30). It is conceivable that a similar mechanism in the hypothalamus or another brain area is taking place as illustrated with the ASTRO-D2KO mouse that lacks D2 in glial cells. Notably, the disruption of the glia D2 pathway partially recapitulated the phenotype of the GLOB-D2KO mouse, including a lower diurnal RQ (Fig. 2C-E) but not a reduced food intake (Fig. F).

As it becomes apparent that D2 plays an important metabolic role in multiple tissues, the development of the FAT-D2KO allowed for a unique insight into the direct role played by D2-generated T3 in BAT physiology. The findings of increased RQ values in these animals indicate a relative state of BAT hypothyroidism despite normal serum T3 levels and provide clear evidence that D2-generated T3 in BAT accelerates fatty acid oxidation. Notably, T3 accelerates fatty acid oxidation by stimulating the expression of rate-limiting elements in this process (32, 54, 55), lowering RQ values (33). However, these experiments frequently involve systemically hypothyroid animals treated with large doses of T3. The evidence obtained in the present study is unique in its physiological context, reflecting the result of D2 inactivation in BAT cells in an otherwise systemically euthyroid animal. Only through this strategy the physiological role played by D2-generated T3 inside BAT cells could be appreciated.

The faster clearance of glucose from the circulation and the increased insulin sensitivity (Fig. H-I) suggest that an increased oxidation of glucose compensates for the impaired fatty acid oxidation in BAT. Whereas this seems to provide sufficient compensation under standard conditions, placing the FAT-D2KO animals on a HFD revealed greater susceptibility to diet-induced obesity (Fig. 4A-D), suggestive of impaired adaptive thermogenesis. This is supported by the observation that at thermoneutrality this phenotype was neutralized (Fig. 4I-L), indicating that the sympathetic nervous system and BAT play an underlying role in this process.

Skeletal muscle expresses very low levels of D2, about two orders of magnitude lower than BAT (26, 56). However, given its large size it is conceivable that D2 contributes significantly to metabolism, similarly to the D2-generated T3 in BAT. The present studies demonstrate that D2 inactivation in skeletal muscle is metabolically neutral, not affecting any of the parameters analyzed, including $VO_2$ and RQ, body weight and composition. In addition, we also increased the metabolic demand by placing these animals on a HFD and their susceptibility to diet-induced obesity was not affect by disruption of D2 activity in skeletal muscle (Fig. 5F-I). Thus, D2-generated T3 in skeletal muscle is not sufficient to play any significant metabolic role.

The analysis of the multiple metabolic parameters and the subsequent adjustments that follow disruption of the D2 pathway - under adverse conditions of environmental temperature and caloric intake - prompt us to speculate what the physiological imperative is, around which all other parameters adjust to. In the present studies, $VO_2$ and EE remained stable in all animal models of global or tissue-specific disruption of the D2-generated T3 mechanism. The present data, and also previously published studies, indicate that localized disruption in thyroid hormone signaling is well neutralized by adjustments in the sympathetic activity while maintaining a stable rate of EE and thermogenesis. Even in systemically hypothyroid mice, an increase in sympathetic activity neutralizes much of the expected metabolic phenotype (57). Thus, given the relatively high surface to volume ratio in mice, EE and thermoregulation seem to be key physiological impera-

tives determining the direction and intensity of the adjustments observed in the present investigation.

D2 is expressed in the human brain, including the hypothalamus (58), as well as BAT that is present in adult individuals (53, 59, 60). This indicates that the present findings are potentially applicable to humans. In fact, a common Dio2 gene polymorphisms has been associated with a number of metabolic conditions, including increased BMI and resistance to insulin (53), supporting the idea that D2 could play a role regulating fatty acid utilization in humans.

In conclusion, the present studies deconstructed the metabolic phenotype exhibited by a mouse with global inactivation of D2, explaining the unexpectedly finding of diurnal acceleration of fatty acid oxidation. The findings in the ASTRO-D2KO mouse indicate that D2-generated T3 in the brain plays a dominant albeit indirect role inhibiting BAT activity and thus slowing down fatty acid oxidation. The findings in the FAT-D2KO mouse, on the contrary, indicate that D2-generated T3 in BAT accelerate fatty acid oxidation, a mechanism that when absent is partially compensated for by an increase in glucose utilization. However, the FAT-D2KO mouse remains susceptible to diet-induce obesity, illustrating how critical this mechanism is. In contrast, the D2 pathway in skeletal muscle is unlikely to play any significant metabolic role. The metabolic characterization of these animal models provides a unique insight into how deiodinase-mediated thyroid hormone signaling is critical for energy homeostasis.

## Acknowledgment

TF, JW and MC conducted experiments, data analyzes, manuscript preparation; BB, GF, EM, DI, CM and AF conducted experiments, data analyzes; BG created the Flox-D2 mouse, reviewed manuscript; A. B. data analyzes, manuscript preparation. The authors are grateful to Professor Carlos Moraes for kindly providing the Cre-MLC mouse used in this study. This work was supported by NIDDK R01 65055 and the European Community's Seventh Framework Program (FP7/2007–2013, no. 259772).

## Disclosure statement

The authors declare no conflict of interest.

## Bibliography

1. Brent, G.A. 2012. Mechanisms of thyroid hormone action. *J Clin Invest* 122:3035-3043.
2. Gereben, B., Zeold, A., Dentice, M., Salvatore, D., and Bianco, A.C. 2008. Activation and inactivation of thyroid hormone by deiodinases: local action with general consequences. *Cell Mol Life Sci* 65:570-590.
3. Callebaut, I., Curcio-Morelli, C., Mornon, J.P., Gereben, B., Buettner, C., Huang, S., Castro, B., Fonseca, T.L., Harney, J.W., Larsen, P.R., et al. 2003. The iodothyronine selenodeiodinases are thioredoxin-fold family proteins containing a glycoside hydrolase clan GH-A-like structure. *J Biol Chem* 278:36887-36896.

4. Bianco, A.C., Salvatore, D., Gereben, B., Berry, M.J., and Larsen, P.R. 2002. Biochemistry, cellular and molecular biology, and physiological roles of the iodothyronine selenodeiodinases. *Endocr Rev* 23:38-89.
5. Hernandez, A., and St Germain, D.L. 2003. Thyroid hormone deiodinases: physiology and clinical disorders. *Curr Opin Pediatr* 15:416-420.
6. Lechan, R.M. 1987. Neuroendocrinology of pituitary hormone regulation. *Endocrinol Metab Clin North Am* 16:475-501.
7. Hall, J.A., Ribich, S., Christoffolete, M.A., Simovic, G., Correa-Medina, M., Patti, M.E., and Bianco, A.C. 2010. Absence of thyroid hormone activation during development underlies a permanent defect in adaptive thermogenesis. *Endocrinology* 151:4573-4582.
8. Medina, M.C., Molina, J., Gadea, Y., Fachado, A., Murillo, M., Simovic, G., Pileggi, A., Hernandez, A., Edlund, H., and Bianco, A.C. 2011. The Thyroid Hormone-Inactivating Type III Deiodinase Is Expressed in Mouse and Human {beta}-Cells and Its Targeted Inactivation Impairs Insulin Secretion. *Endocrinology*.
9. Ueta, C.B., Oskouei, B.N., Olivares, E.L., Pinto, J.R., Correa, M.M., Simovic, G., Simonides, W.S., Hare, J.M., and Bianco, A.C. 2012. Absence of myocardial thyroid hormone inactivating deiodinase results in restrictive cardiomyopathy in mice. *Mol Endocrinol* 26:809-818.
10. Dentice, M., Marsili, A., Ambrosio, R., Guardiola, O., Sibilio, A., Paik, J.H., Minchiotti, G., DePinho, R.A., Fenzi, G., Larsen, P.R., et al. 2010. The FoxO3/type 2 deiodinase pathway is required for normal mouse myogenesis and muscle regeneration. *J Clin Invest* 120:4021-4030.
11. Gereben, B., Zavacki, A.M., Ribich, S., Kim, B.W., Huang, S.A., Simonides, W.S., Zeold, A., and Bianco, A.C. 2008. Cellular and molecular basis of deiodinase-regulated thyroid hormone signaling. *Endocr Rev* 29:898-938.
12. Hernandez, A., Morte, B., Belinchon, M.M., Ceballos, A., and Bernal, J. 2012. Critical role of types 2 and 3 deiodinases in the negative regulation of gene expression by t3 in the mouse cerebral cortex. *Endocrinology* 153:2919-2928.
13. Castillo, M., Hall, J.A., Correa-Medina, M., Ueta, C., Won Kang, H., Cohen, D.E., and Bianco, A.C. 2011. Disruption of thyroid hormone activation in type 2 deiodinase knockout mice causes obesity with glucose intolerance and liver steatosis only at thermoneutrality. *Diabetes* 60:1082-1089.
14. Feldmann, H.M., Golozoubova, V., Cannon, B., and Nedergaard, J. 2009. UCP1 ablation induces obesity and abolishes diet-induced thermogenesis in mice exempt from thermal stress by living at thermoneutrality. *Cell Metab* 9:203-209.
15. Ueta, C.B., Olivares, E.L., and Bianco, A.C. 2011. Responsiveness to Thyroid Hormone and to Ambient Temperature Underlies Differences Between Brown Adipose Tissue and Skeletal Muscle Thermogenesis in a Mouse Model of Diet-Induced Obesity. *Endocrinology*.
16. Bianco, A.C., Carvalho, S.D., Carvalho, C.R., Rabelo, R., and Moriscot, A.S. 1998. Thyroxine 5'-deiodination mediates norepinephrine-induced lipogenesis in dispersed brown adipocytes. *Endocrinology* 139:571-578.
17. Castillo, M., Hall, J.A., Correa-Medina, M., Ueta, C., Kang, H.W., Cohen, D.E., and Bianco, A.C. 2011. Disruption of thyroid hormone activation in type 2 deiodinase knockout mice causes obesity with glucose intolerance and liver steatosis only at thermoneutrality. *Diabetes* 60:1082-1089.
18. Bianco, A.C., Kieffer, J.D., and Silva, J.E. 1992. Adenosine 3',5'-monophosphate and thyroid hormone control of uncoupling protein messenger ribonucleic acid in freshly dispersed brown adipocytes. *Endocrinology* 130:2625-2633.

19. Bianco, A.C., Sheng, X.Y., and Silva, J.E. 1988. Triiodothyronine amplifies norepinephrine stimulation of uncoupling protein gene transcription by a mechanism not requiring protein synthesis. *J Biol Chem* 263:18168-18175.
20. Branco, M., Ribeiro, M., Negrao, N., and Bianco, A.C. 1999. 3,5,3'-Triiodothyronine actively stimulates UCP in brown fat under minimal sympathetic activity. *Am J Physiol* 276:E179-187.
21. de Jesus, L.A., Carvalho, S.D., Ribeiro, M.O., Schneider, M., Kim, S.W., Harney, J.W., Larsen, P.R., and Bianco, A.C. 2001. The type 2 iodothyronine deiodinase is essential for adaptive thermogenesis in brown adipose tissue. *J Clin Invest* 108:1379-1385.
22. Christoffolete, M.A., Linardi, C.C., de Jesus, L., Ebina, K.N., Carvalho, S.D., Ribeiro, M.O., Rabelo, R., Curcio, C., Martins, L., Kimura, E.T., et al. 2004. Mice with targeted disruption of the Dio2 gene have cold-induced overexpression of the uncoupling protein 1 gene but fail to increase brown adipose tissue lipogenesis and adaptive thermogenesis. *Diabetes* 53:577-584.
23. Bianco, A.C., and Silva, J.E. 1988. Cold exposure rapidly induces virtual saturation of brown adipose tissue nuclear T3 receptors. *Am J Physiol* 255:E496-503.
24. Carvalho, S.D., Kimura, E.T., Bianco, A.C., and Silva, J.E. 1991. Central role of brown adipose tissue thyroxine 5'-deiodinase on thyroid hormone-dependent thermogenic response to cold. *Endocrinology* 128:2149-2159.
25. Crantz, F.R., and Larsen, P.R. 1980. Rapid thyroxine to 3,5,3'-triiodothyronine conversion and nuclear 3,5,3'-triiodothyronine binding in rat cerebral cortex and cerebellum. *Journal of Clinical Investigation* 65:935-938.
26. Grozovsky, R., Ribich, S., Rosene, M.L., Mulcahey, M.A., Huang, S.A., Patti, M.E., Bianco, A.C., and Kim, B.W. 2009. Type 2 deiodinase expression is induced by peroxisomal proliferator-activated receptor-gamma agonists in skeletal myocytes. *Endocrinology* 150:1976-1983.
27. Gouveia, C.H., Christoffolete, M.A., Zaitune, C.R., Dora, J.M., Harney, J.W., Maia, A.L., and Bianco, A.C. 2005. Type 2 iodothyronine selenodeiodinase is expressed throughout the mouse skeleton and in the MC3T3-E1 mouse osteoblastic cell line during differentiation. *Endocrinology* 146:195-200.
28. Guadano-Ferraz, A., Obregon, M.J., St Germain, D.L., and Bernal, J. 1997. The type 2 iodothyronine deiodinase is expressed primarily in glial cells in the neonatal rat brain. *Proc Natl Acad Sci U S A* 94:10391-10396.
29. Tu, H.M., Kim, S.W., Salvatore, D., Bartha, T., Legradi, G., Larsen, P.R., and Lechan, R.M. 1997. Regional distribution of type 2 thyroxine deiodinase messenger ribonucleic acid in rat hypothalamus and pituitary and its regulation by thyroid hormone. *Endocrinology* 138:3359-3368.
30. Coppola, A., Liu, Z.W., Andrews, Z.B., Paradis, E., Roy, M.C., Friedman, J.M., Ricquier, D., Richard, D., Horvath, T.L., Gao, X.B., et al. 2007. A central thermogenic-like mechanism in feeding regulation: an interplay between arcuate nucleus T3 and UCP2. *Cell Metab* 5:21-33.
31. Fekete, C., Gereben, B., Doleschall, M., Harney, J.W., Dora, J.M., Bianco, A.C., Sarkar, S., Liposits, Z., Rand, W., Emerson, C., et al. 2004. Lipopolysaccharide induces type 2 iodothyronine deiodinase in the mediobasal hypothalamus: implications for the nonthyroidal illness syndrome. *Endocrinology* 145:1649-1655.
32. 1972. Fatty acid metabolism in rats treated with triiodothyronine. *Nutr Rev* 30:234-236.
33. Smith, D.C., and Brown, F.C. 1952. The effect of parrot fish thyroid extract on the respiratory metabolism of the white rat. *Biological Bulletin* 102:278-286.
34. Marsili, A., Aguayo-Mazzucato, C., Chen, T., Kumar, A., Chung, M., Lunsford, E.P., Harney, J.W., Van-Tran, T., Gianetti, E., Ramadan, W., et al. 2011. Mice with a targeted deletion of the type 2 deiodinase are insulin resistant and susceptible to diet induced obesity. *PLoS One* 6:e20832.

35. Cryer, P.E. 2008. Glucose homeostasis and hypoglycemia. In *Williams Textbook of Endocrinology* Saunders. 1503-1533.
36. Bianco, A.C., Anderson, G., Forrest, D., Galton, V.A., Gereben, B., Kim, B.W., Kopp, P.A., Liao, X.H., Obregon, M.J., Peeters, R.P., et al. 2014. American thyroid association guide to investigating thyroid hormone economy and action in rodent and cell models. *Thyroid* 24:88-168.
37. Fonseca, T.L., Correa-Medina, M., Campos, M.P., Wittmann, G., Werneck-de-Castro, J.P., Drigo, R.A., Mora-Garzon, M., Ueta, C.B., Caicedo, A., Fekete, C., et al. 2013. Coordination of hypothalamic and pituitary T3 production regulates TSH expression. *J Clin Invest* 123:1492-1500.
38. Westholm, D.E., Marold, J.D., Viken, K.J., Duerst, A.H., Anderson, G.W., and Rumbley, J.N. 2010. Evidence of evolutionary conservation of function between the thyroxine transporter Oatp1c1 and major facilitator superfamily members. *Endocrinology* 151:5941-5951.
39. Zhuo, L., Theis, M., Alvarez-Maya, I., Brenner, M., Willecke, K., and Messing, A. 2001. hGFAP-cre transgenic mice for manipulation of glial and neuronal function in vivo. *Genesis* 31:85-94.
40. Alkemade, A., Unmehopa, U.A., Wiersinga, W.M., Swaab, D.F., and Fliers, E. 2005. Glucocorticoids decrease thyrotropin-releasing hormone messenger ribonucleic acid expression in the paraventricular nucleus of the human hypothalamus. *J Clin Endocrinol Metab* 90:323-327.
41. Lusk, G. 1926. Animal Calorimetry. Analysis of the oxidation of mixtures of carbohydrates and fat. *The journal of Biology Chemistry* 124:41-42.
42. Medina, M.C., Molina, J., Gadea, Y., Fachado, A., Murillo, M., Simovic, G., Pileggi, A., Hernandez, A., Edlund, H., and Bianco, A.C. 2011. The thyroid hormone-inactivating type III deiodinase is expressed in mouse and human beta-cells and its targeted inactivation impairs insulin secretion. *Endocrinology* 152:3717-3727.
43. Christoffolete, M.A., Ribeiro, R., Singru, P., Fekete, C., da Silva, W.S., Gordon, D.F., Huang, S.A., Crescenzi, A., Harney, J.W., Ridgway, E.C., et al. 2006. Atypical expression of type 2 iodothyronine deiodinase in thyrotrophs explains the thyroxine-mediated pituitary thyrotropin feedback mechanism. *Endocrinology* 147:1735-1743.
44. Curcio-Morelli, C., Gereben, B., Zavacki, A.M., Kim, B.W., Huang, S., Harney, J.W., Larsen, P.R., and Bianco, A.C. 2003. In vivo dimerization of types 1, 2, and 3 iodothyronine selenodeiodinases. *Endocrinology* 144:937-946.
45. Diano, S., Naftolin, F., Goglia, F., and Horvath, T.L. 1998. Fasting-induced increase in type II iodothyronine deiodinase activity and messenger ribonucleic acid levels is not reversed by thyroxine in the rat hypothalamus. *Endocrinology* 139:2879-2884.
46. Fekete, C., Singru, P.S., Sanchez, E., Sarkar, S., Christoffolete, M.A., Riberio, R.S., Rand, W.M., Emerson, C.H., Bianco, A.C., and Lechan, R.M. 2006. Differential effects of central leptin, insulin, or glucose administration during fasting on the hypothalamic-pituitary-thyroid axis and feeding-related neurons in the arcuate nucleus. *Endocrinology* 147:520-529.
47. Bianco, A.C., and Silva, J.E. 1987. Optimal response of key enzymes and uncoupling protein to cold in BAT depends on local T3 generation. *Am J Physiol* 253:E255-263.
48. Carvalho, S.D., Negrao, N., and Bianco, A.C. 1993. Hormonal regulation of malic enzyme and glucose-6-phosphate dehydrogenase in brown adipose tissue. *Am J Physiol* 264:E874-881.
49. Werneck de Castro, J.P., Fonseca, T.L., Ignacio, D.L., Fernandes, G.W., Baldanza, M.R., Rangel, I.F., Balazs, G.B., Miranda, M.F., Andrade, C., Bianco, A.C., et al. 2013. Both skeletal myocytes and adipocytes express the type 2 deiodinase within skeletal muscle. In *83rd Annual Meeting of the Americam Thyroid Association*. San Juan, Porto Rico: American Thyroid Association 69.

50. Lopez, M., Varela, L., Vazquez, M.J., Rodriguez-Cuenca, S., Gonzalez, C.R., Velagapudi, V.R., Morgan, D.A., Schoenmakers, E., Agassandian, K., Lage, R., et al. 2010. Hypothalamic AMPK and fatty acid metabolism mediate thyroid regulation of energy balance. *Nat Med* 16:1001-1008.
51. Morrison, S.F., Madden, C.J., and Tupone, D. 2012. Central control of brown adipose tissue thermogenesis. *Front Endocrinol (Lausanne)* 3.
52. Mittag, J., Lyons, D.J., Sallstrom, J., Vujovic, M., Dudazy-Gralla, S., Warner, A., Wallis, K., Alkemade, A., Nordstrom, K., Monyer, H., et al. 2013. Thyroid hormone is required for hypothalamic neurons regulating cardiovascular functions. *J Clin Invest* 123:509-516.
53. Bianco, A.C., and Mcaninch, E.A. 2013. The role of thyroid hormone and brown adipose tissue in energy homeostasis. *The Lancet Diabetes & Endocrinology* 1:250-258.
54. Stakkestad, J.A., and Bremer, J. 1982. The metabolism of fatty acids in hepatocytes isolated from triiodothyronine-treated rats. *Biochim Biophys Acta* 711:90-100.
55. Stakkestad, J.A., and Bremer, J. 1983. The outer carnitine palmitoyltransferase and regulation of fatty acid metabolism in rat liver in different thyroid states. *Biochim Biophys Acta* 750:244-252.
56. Ramadan, W., Marsili, A., Huang, S., Larsen, P.R., and Silva, J.E. 2011. Type-2 iodothyronine 5'deiodinase in skeletal muscle of C57BL/6 mice. I. Identity, subcellular localization, and characterization. *Endocrinology* 152:3082-3092.
57. Ueta, C.B., Olivares, E.L., and Bianco, A.C. 2011. Responsiveness to thyroid hormone and to ambient temperature underlies differences between brown adipose tissue and skeletal muscle thermogenesis in a mouse model of diet-induced obesity. *Endocrinology* 152:3571-3581.
58. Campos-Barros, A., Hoell, T., Musa, A., Sampaolo, S., Stoltenburg, G., Pinna, G., Eravci, M., Meinhold, H., and Baumgartner, A. 1996. Phenolic and tyrosyl ring iodothyronine deiodination and thyroid hormone concentrations in the human central nervous system. *The Journal of Clinical Endocrinology and Metabolism* 81:2179-2185.
59. Cypess, A.M., White, A.P., Vernochet, C., Schulz, T.J., Xue, R., Sass, C.A., Huang, T.L., Roberts-Toler, C., Weiner, L.S., Sze, C., et al. 2013. Anatomical localization, gene expression profiling and functional characterization of adult human neck brown fat. *Nat Med* 19:635-639.
60. Virtanen, K.A., Lidell, M.E., Orava, J., Heglind, M., Westergren, R., Niemi, T., Taittonen, M., Laine, J., Savisto, N.J., Enerback, S., et al. 2009. Functional brown adipose tissue in healthy adults. *N Engl J Med* 360:1518-1525.

**Legend to the figures**

**Figure 1- Metabolic phenotype of the GLOB-D2KO mouse.** GLOB-D2KO and WT controls were acclimated to individual metabolic cages in the comprehensive lab animal monitoring system (C.L.A.M.S.) for 48 hours before measurements were recorded. **A)** Oxygen consumption ($VO_2$) during 12h light and dark cycles recorded at the second day after acclimatization; **B)** Same as in A, except that what is shown is Respiratory quotient (RQ); **C)** Contribution of fat oxidation to daily energy expenditure during the light cycle; **D)** Food intake during light and dark cycles of animals kept on regular chow diet at room temperature (22$^o$C); **E)** $VO_2$ during 12h light and dark cycles recorded during acute cold (4$^o$C) exposure; **F)** Same as in E, except that what is shown is RQ; **G)** Food intake during light and dark cycles of animals kept on regular chow diet during the period of cold (4$^o$C) exposure; **H)** $VO_2$ register during chronically (15 days) cold exposed where the environment temperature was gradually and progressively decreased every 3-4 days; **I)** Same as in H, except that what is shown is RQ; **J)** $VO_2$ during 12h light and dark cycles recorded on the first day of 48hs of fasting and **K)** Same as in J, except that what is shown is RQ. Entries are mean ± SEM of 3-7 animals. Area under the curve (AUC) was calculated during light and dark cycles for each individual animal. Statistical significance is shown in each graph and was set as $p < 0.05$. Student's t test was used to compare WT and GLOB-D2KO groups within treatment conditions. Black horizontal bars denote the dark period of day (12hs).

**Figure 2- Metabolic phenotype of the ASTRO-D2KO mouse kept on regular chow diet at room temperature (22$^o$C). A)** Body weight evolution during 2 months period; **B)** Body weight of the animals right before admission to C.L.A.M.S.; **C)** Body composition measured by DEXA 48h before the animals were admit to C.L.A.M.S.; **D)** $VO_2$ during 12h light and dark cycles; ASTRO-D2KO mouse and controls were acclimated to individual metabolic cages in the C.L.A.M.S. for 48 hours before measurements were recorded; data shown is the second day after acclimatization; **E)** Same as in D, except that what is shown is RQ; **F)** Contribution of fat oxidation to daily energy expenditure during the light cycle and **G)** Food intake of the same animals during light and dark cycles. Entries are mean ± SEM of 4-5 animals. Area under the curve (AUC) was calculated during light and dark cycles for each individual animal. Statistical significance is shown in each graph and was set as $p < 0.05$. Student's t test was used to compare controls and ASTRO-D2KO groups within treatment conditions. Black horizontal bars denote the dark period of day (12hs).

**Figure 3- Metabolic phenotype of the FAT-D2KO mouse kept on regular chow diet. A)** Body weight evolution during 5 months period of animals kept at room temperature (22$^o$C). The FAT-D2KO mouse and controls were acclimated to individual metabolic cages in the C.L.A.M.S. for 48 hours before measurements were recorded; **B)** Body weight of the animals right before the animals were admit to C.L.A.M.S.; **C)** Body composition measured by DEXA 48h before the animals were admit to C.L.A.M.S.; **D)** $VO_2$ during 12h light and dark cycles recorded at the second day after acclimatization of animals kept on regular chow diet at room temperature (22$^o$C); **E)** Same as in D, except that what is shown is RQ; **F)** Contribution of fat oxidation to daily energy expenditure during the light cycle in the same animals; **G)** Food intake during light and dark cycles in the same animals; **H)** Blood glucose concentrations at the indicated time points after ip glucose injection (2g/kg) in 2-month-old FAT-D2KO and controls animals; **I)** Blood glucose concentration at the indicated time points before and after ip injection of regu-

lar human insulin (0.75 U/kg body weight) in 2-month-old FAT-D2KO and control animals; **J)** $VO_2$ during 12h light and dark cycles recorded during chronic (15 days) exposure to thermoneutrality (30$^o$C); **K)** Same as in E, except that what is shown is RQ; **L)** Food intake during light and dark cycles of animals kept at thermoneutrality; **M)** $VO_2$ during 12h light and dark cycles recorded on the first day of 48hs of fasting and **N)** Same as in J, except that what is shown is RQ. Entries are mean ± SEM of 5-12 animals. Area under the curve (AUC) was calculated during light and dark cycles for each individual animal. Statistical significance is shown in each graph and was set as $p < 0.05$. Student's t test was used to compare controls and FAT-D2KO groups within treatment conditions. Black horizontal bars denote the dark period of day (12hs). (*, $p<0.05$; **, $p<0.01$ and ***, $p<0.001$ vs. control).

**Figure 4- Effect of high-fat diet (HFD) in the FAT-D2KO mice at room temperature and thermoneutrality.** The FAT-D2KO and controls were fed with HFD for 8 weeks. **A)** Body weight evolution during 8 weeks of treatment of animals kept at room temperature (22$^o$C); **B)** Area under the curve from the BW shown in A was calculated from each individual animal; **C)** Food intake during light and dark cycles in the same animals; **D)** Body composition measured by DEXA in the animals kept at room temperature before (day 1) and after (day 60) HFD; **E)** Delta % of fat measured by DEXA in D, calculated by the difference between days 1 and 60; **F)** Contribution of fat oxidation to daily energy expenditure during the light cycle in the same animals; **G)** $VO_2$ during 12h light and dark cycles in the animals kept at room temperature after 8 weeks on HFD; The FAT-D2KO mouse and controls were acclimated to individual metabolic cages in the C.L.A.M.S. for 48 hours before measurements were recorded; data shown is the second day after acclimatization; **H)** Same as in G, except that what is shown is RQ; **I)** Body weight evolution during 8 weeks of treatment of animals kept at thermoneutrality (30$^o$C); **J)** Area under the curve from the BW represented in the figure I, calculated from each individual animal; **K)** Food intake during light and dark cycles in the same animals; **L)** Body composition measured by DEXA in the animals kept at thermoneutrality before (day 1) and after (day 60) HFD; **M)** Delta % of fat measured by DEXA in L, calculated by the difference between days 1 and 60; **N)** Contribution of fat oxidation to daily energy expenditure during the light cycle in the same animals; and **O)** $VO_2$ during 12h light and dark cycles in the animals kept at thermoneutrality after 8 weeks on the HFD; **P)** Same as in O, except that what is shown is RQ; Entries are mean ± SEM of 5-6 animals. Statistical significance is shown in each graph and was set as $p < 0.05$. Student's t test was used to compare controls and FAT-D2KO groups within treatment conditions. Black horizontal bars denote the dark period of day (12hs).

**Figure 5- Metabolic phenotype of the SKM-D2KO mouse kept on regular chow diet and HFD at room temperature (22$^o$C). A)** Body weight evolution during 2 months period; **B)** Body weight of the animals right before admission to C.L.A.M.S.; **C)** Body composition measured by DEXA 48h before the animals were admit to C.L.A.M.S.; **D)** $VO_2$ during 12h light and dark cycles; SKM-D2KO mouse and controls were acclimated to individual metabolic cages in the C.L.A.M.S. for 48 hours before measurements were recorded; data shown is the second day after acclimatization; **E)** Same as in D, except that what is shown is RQ; **F)** Contribution of fat oxidation to daily energy expenditure during the light cycle; **G)** Food intake of the same animals during light and dark cycles; **H)** Body weight evolution during 8 weeks of treatment with HFD in animals kept at room temperature (22$^o$C); **I)** Area under the curve from the BW represented in

the figure H, calculated from each individual animal; **J)** Body composition measured by DEXA in the animals kept at room temperature before (day 1) and after (day 60) HFD; **K)** Delta % of fat measured by DEXA in J, calculated by the difference between days 1 and 60; **L)** $VO_2$ during 12h light and dark cycles in the animals kept at room temperature after 8 weeks on HFD; The SKM-D2KO mouse and controls were acclimated to individual metabolic cages in the C.L.A.M.S. for 48 hours before measurements were recorded; data shown is the second day after acclimatization and **M)** Same as in E, except that what is shown is RQ; Entries are mean ± SEM of 3-6 animals. Statistical significance is shown in each graph and was set as $p < 0.05$. Student's t test was used to compare controls and SKM-D2KO groups within treatment conditions. Black horizontal bars denote the dark period of day (12hs).

Figure 1

## ROOM TEMPERATURE

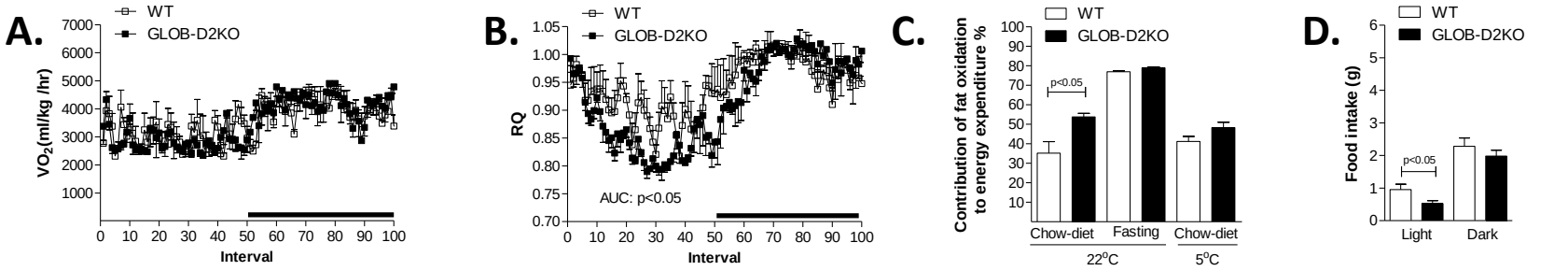


## ACUTE COLD EXPOSURE – 24 HOURS

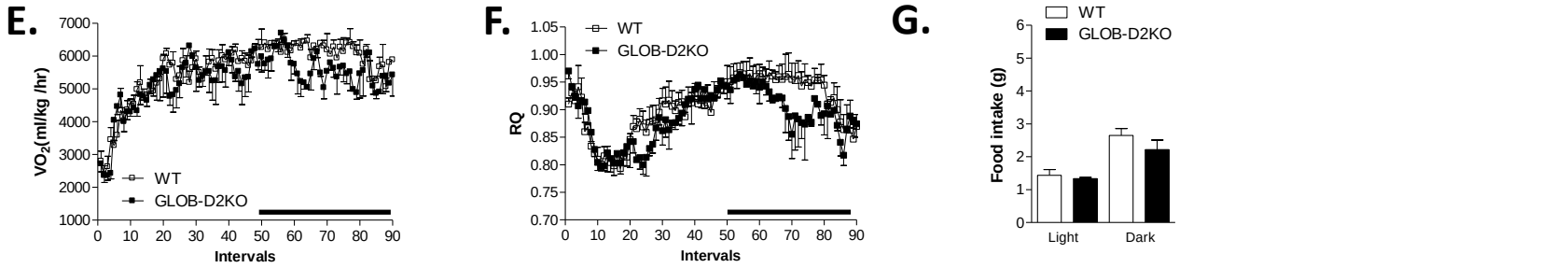


## CHRONIC COLD EXPOSURE – 15 DAYS

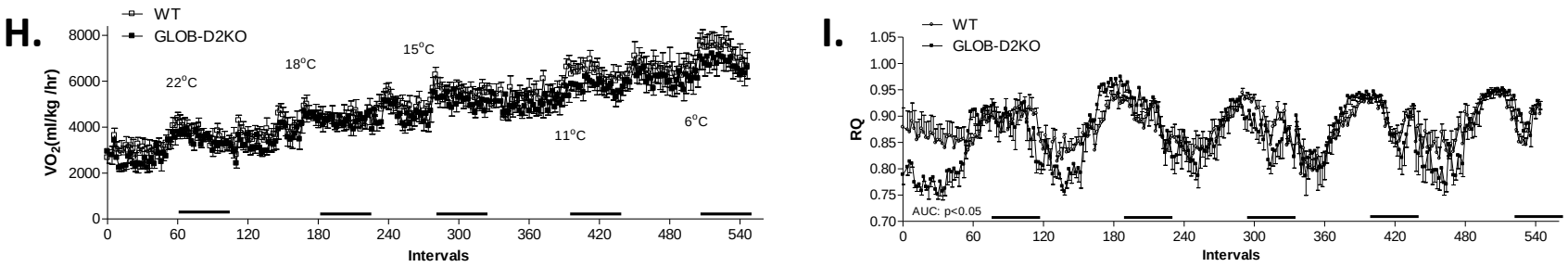


## FASTING – 48 HOURS

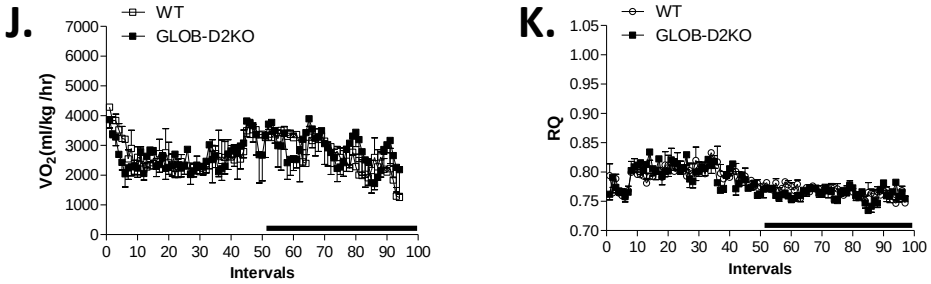

# Figure 2

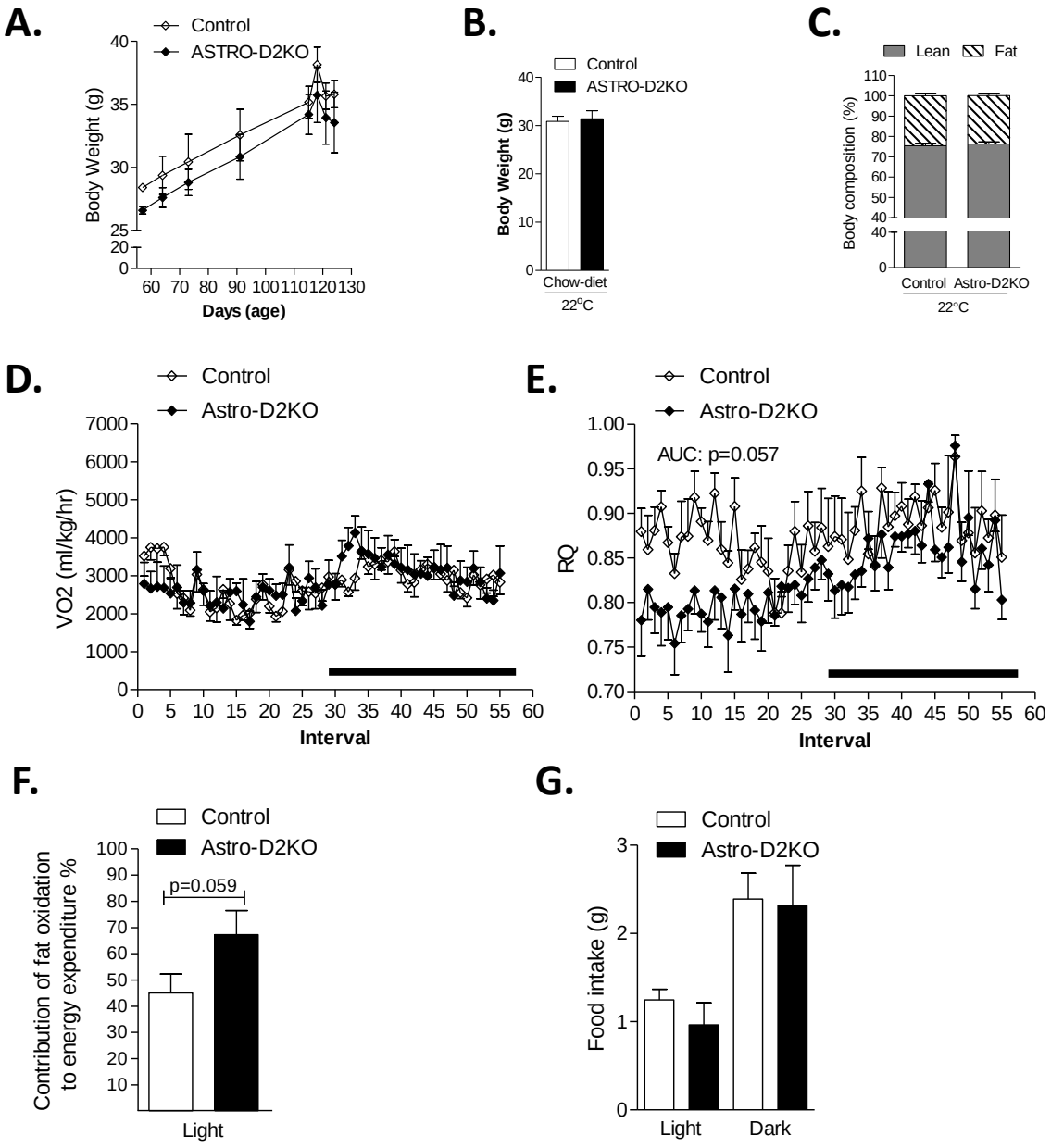
A.
Control
ASTRO-D2KO
Body Weight (g)
Days (age)
B.
Control
ASTRO-D2KO
Body Weight (g)
Chow-diet
22°C
C.
Lean
Fat
Body composition (%)
Control
Astro-D2KO
22°C
D.
Control
Astro-D2KO
VO2 (ml/kg/hr)
Interval
E.
Control
Astro-D2KO
AUC: p=0.057
RQ
Interval
F.
Control
Astro-D2KO
p=0.059
Contribution of fat oxidation to energy expenditure %
Light
G.
Control
Astro-D2KO
Food intake (g)
Light
Dark

ROOM TEMPERATURE

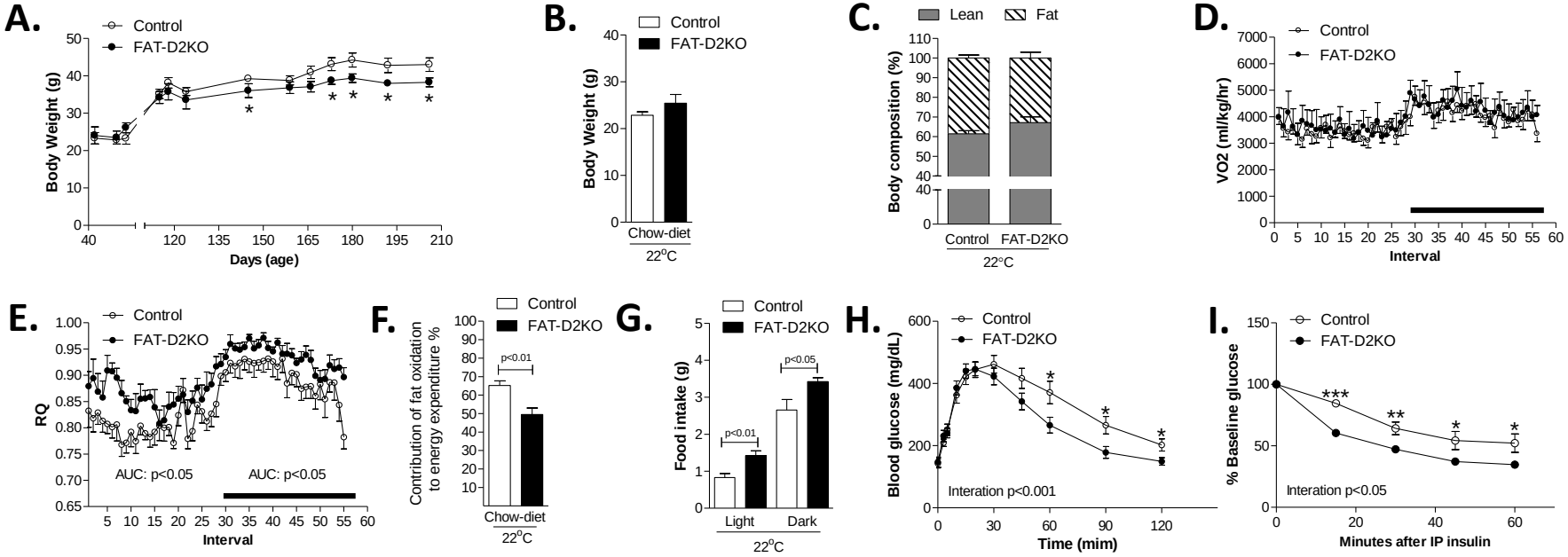


THERMONEUTRALITY – 60 DAYS

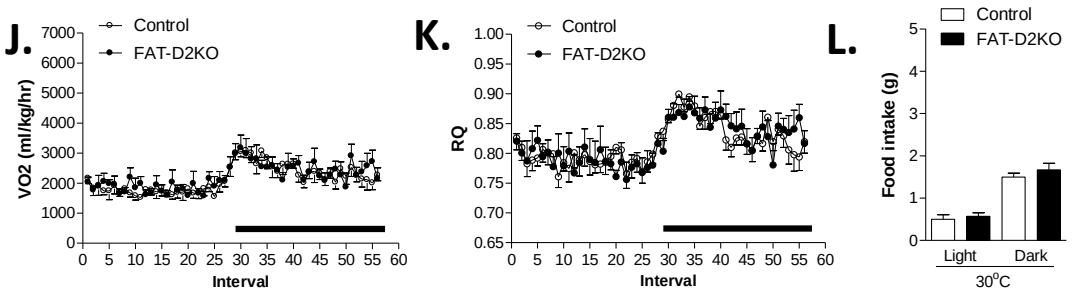


FASTING – 48 HOURS

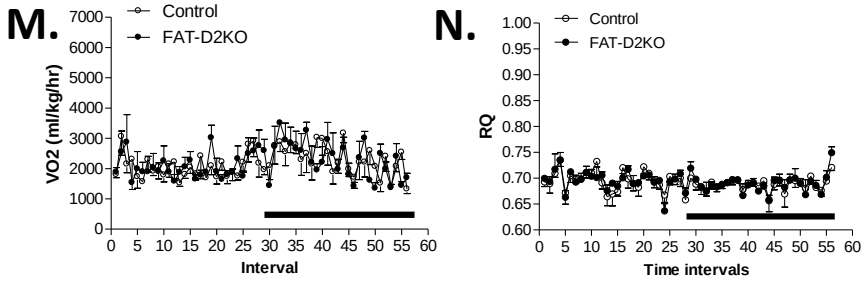


**Figure 3**

# Figure 4

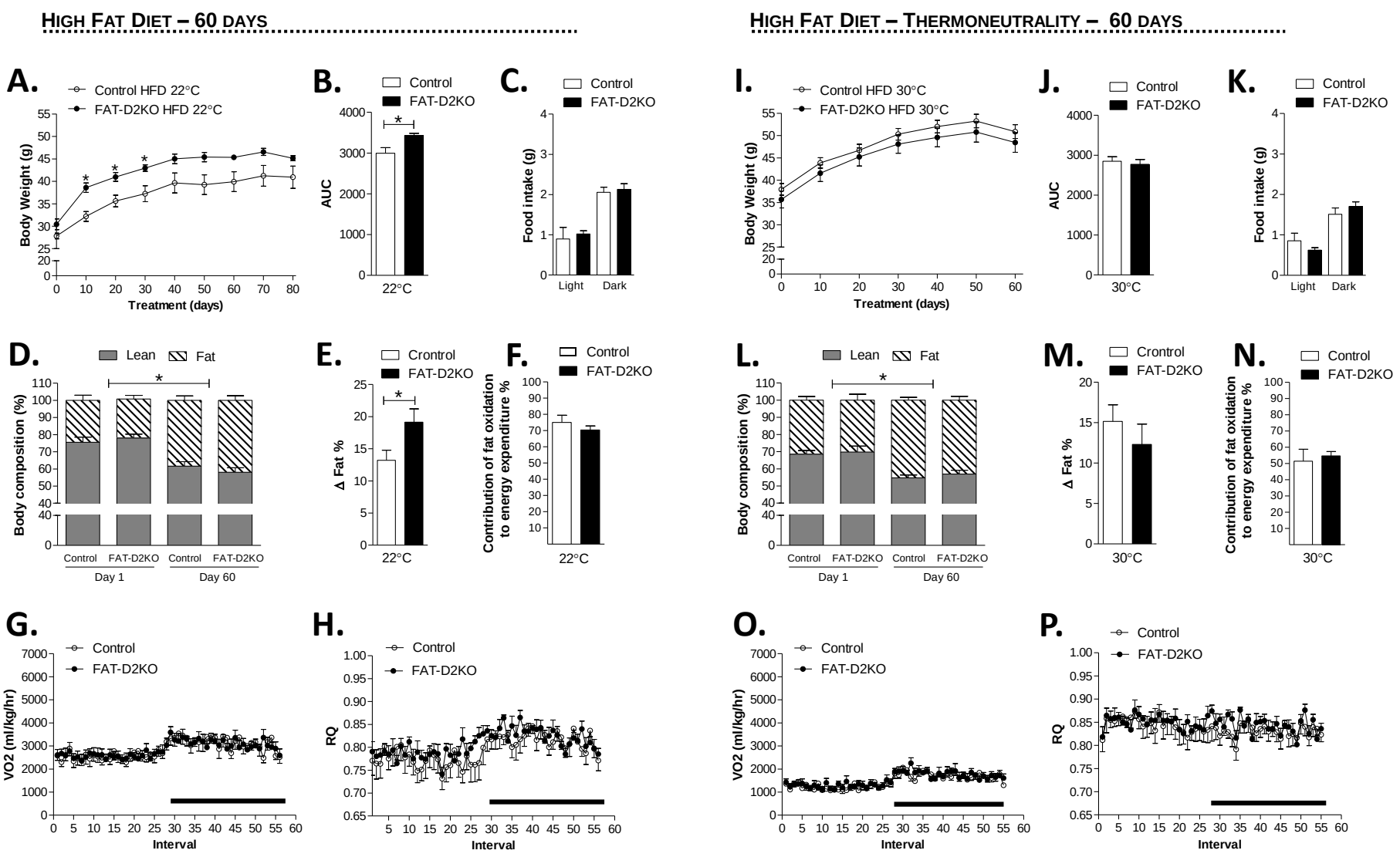
HIGH FAT DIET – 60 DAYS
HIGH FAT DIET – THERMONEUTRALITY – 60 DAYS
A.
Control HFD 22°C
FAT-D2KO HFD 22°C
Body Weight (g)
Treatment (days)
B.
Control
FAT-D2KO
AUC
22°C
C.
Control
FAT-D2KO
Food intake (g)
Light
Dark
I.
Control HFD 30°C
FAT-D2KO HFD 30°C
Body Weight (g)
Treatment (days)
J.
Control
FAT-D2KO
AUC
30°C
K.
Control
FAT-D2KO
Food intake (g)
Light
Dark
D.
Lean
Fat
Body composition (%)
Control
FAT-D2KO
Control
FAT-D2KO
Day 1
Day 60
E.
Crontrol
FAT-D2KO
Δ Fat %
22°C
F.
Control
FAT-D2KO
Contribution of fat oxidation to energy expenditure %
22°C
L.
Lean
Fat
Body composition (%)
Control
FAT-D2KO
Control
FAT-D2KO
Day 1
Day 60
M.
Crontrol
FAT-D2KO
Δ Fat %
30°C
N.
Control
FAT-D2KO
Contribution of fat oxidation to energy expenditure %
30°C
G.
Control
FAT-D2KO
VO2 (ml/kg/hr)
Interval
H.
Control
FAT-D2KO
RQ
Interval
O.
Control
FAT-D2KO
VO2 (ml/kg/hr)
Interval
P.
Control
FAT-D2KO
RQ
Interval

Figure 5

ROOM TEMPERATURE

HIGH FAT DIET – 60 DAYS

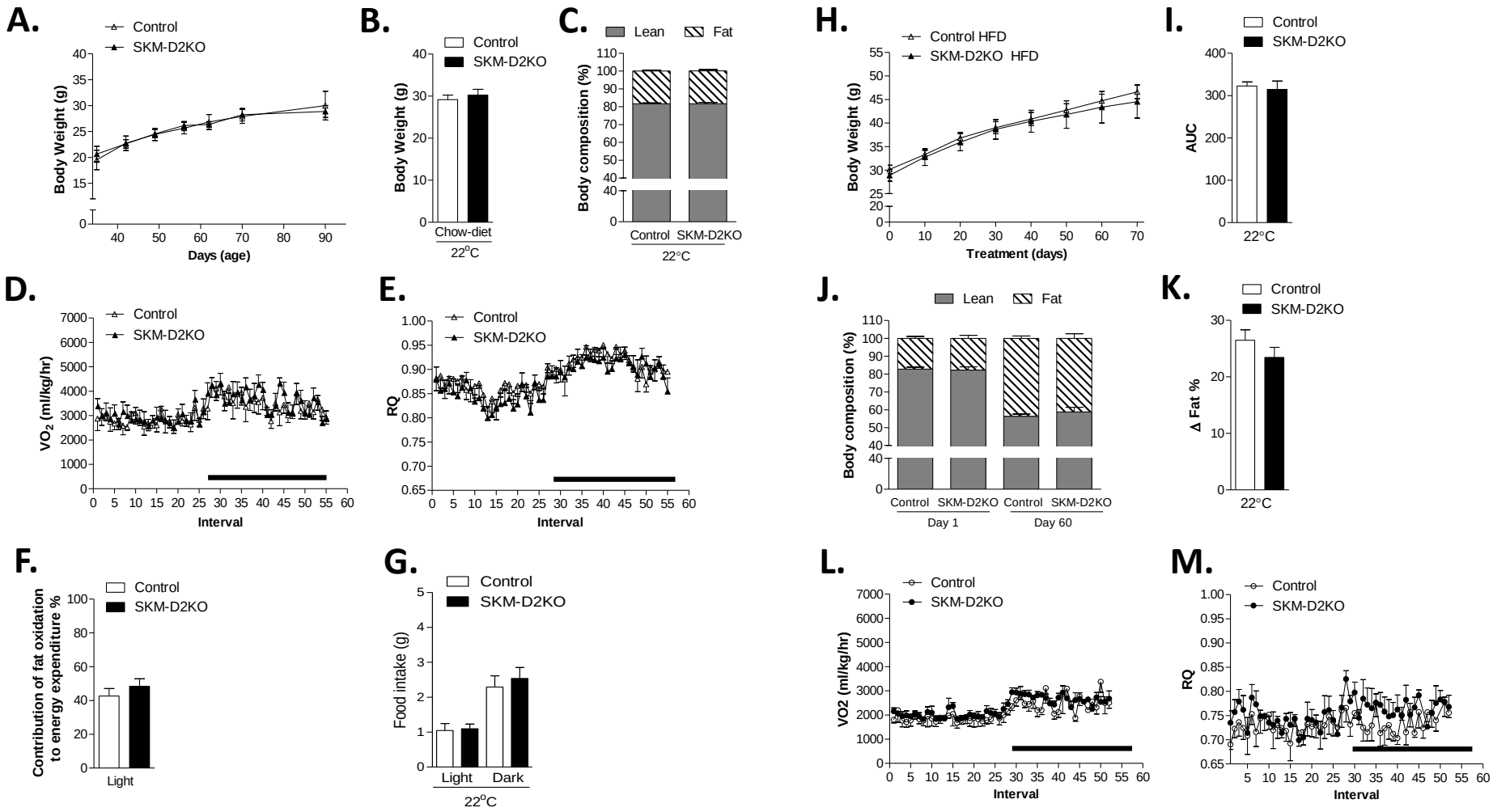

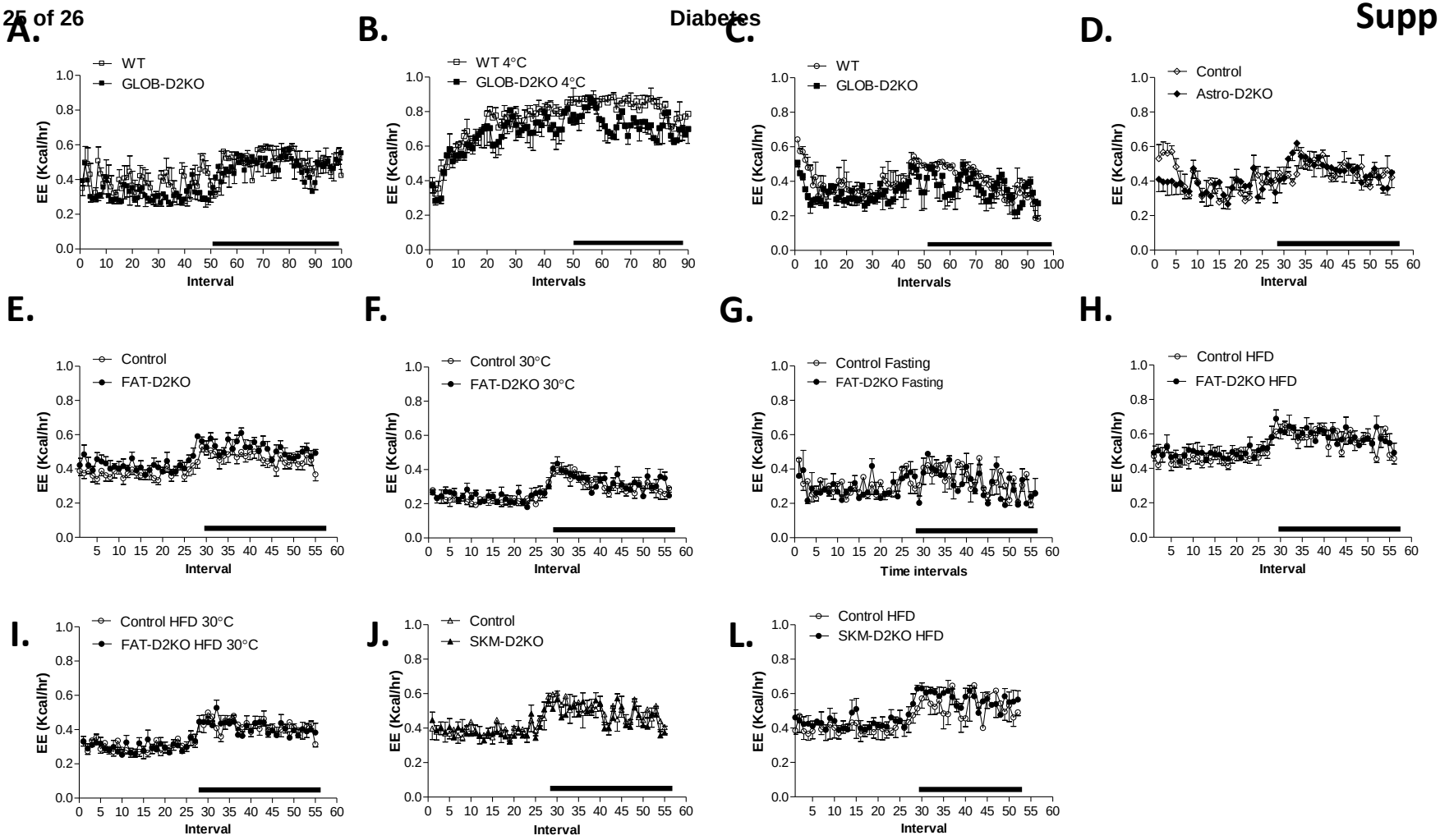


**Supplemental Figure 1- Energy expenditure (EE) in GLOB-D2KO, ASTRO-D2KO, FAT-D2KO and SKM-D2KO measured under different conditions.** The KO and WT controls were acclimated to individual metabolic cages in the comprehensive lab animal monitoring system (C.L.A.M.S.) for 48 hours before measurements were recorded. **A)** Energy expenditure (EE) during 12h light and dark cycles recorded on the second day after acclimatization in the GLOB-D2KO and WT mice at room temperature; **B)** Same as in A, except measurements were recorded during acute cold (4ºC) exposure of 24hs duration; **C)** Same as in A, except measurements were recorded on the first day of a 48hs interval of fasting; **D)** EE in the ASTRO-D2KO and controls at room temperature; **E)** EE in the FAT-D2KO and controls at room temperature; **F)** Same as in E, except measurements were recorded during chronic (15 days) exposure to thermoneutrality (30ºC); **G)** Same as in E, except measurements were recorded on the first day of a 48hs interval of fasting; **H)** Same as in E, except measurements were recorded in the animals kept at room temperature after 8 weeks on HFD; **I)** Same as in H, however the animals were kept at thermoneutrality (30ºC); **J)** EE in the SMK-D2KO and controls at room temperature; **L)** Same as in J, except measurements were recorded in the animals kept at room temperature after 8 weeks on HFD; Entries are mean ± SEM. Statistical significance is shown in each graph and was set as $p < 0.05$. Student's t test was used to compare KO animals and the respective controls.

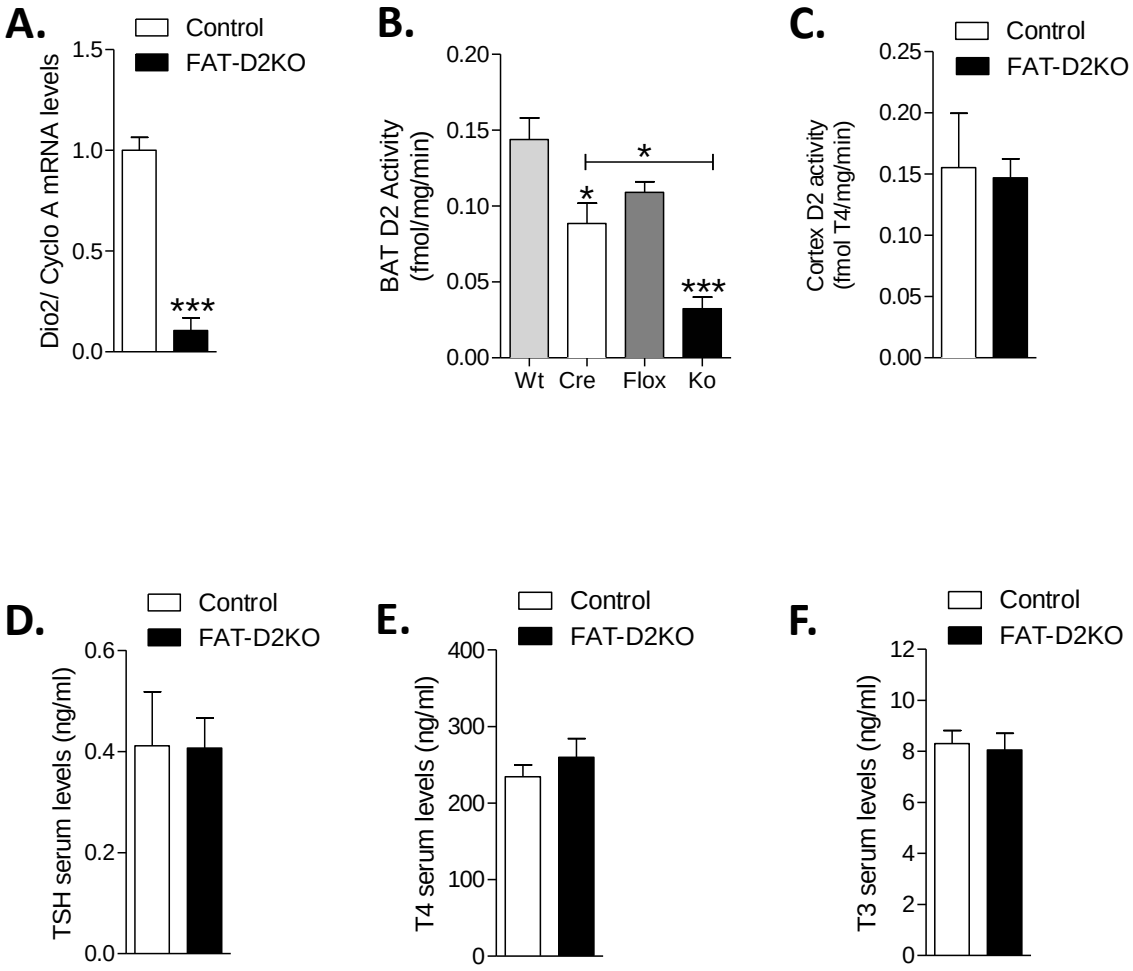


**Supplemental figure 2**- Characterization of FAT-D2KO mouse. **A)** Dio2 expression in the BAT of FAT-D2KO mouse and Controls (n=5) ; **B)** D2 activity in sonicate of BAT in WT, Cre Fabp4, FloxD2 and FAT-D2KO mouse (n=4-6); **C)** D2 activity in sonicate of cortex in control and FAT-D2KO mouse (n=4) and **D)** Serum TSH, **E)** T4 and **F)** T3 levels of control and Fat-D2KO mice (n=10-11). Entries are mean ± SEM. Statistical significance is shown in each graph and was set as $p < 0.05$. Student's t test was used to compare controls and FAT-D2KO. (*, $p<0.05$ and ***, $p<0.001$ vs. control).